CONF

CONF-811140--23

THE POLOIDAL FIELD-COIL SYSTEM OF THE FUSION-ENGINEERING DEVICE*

D. J. Strickler and Y-K. M. Peng
Oak Ridge National Laboratory
Oak Ridge, Tennessee 37830

Draft

Introduction

The Fusion Engineering Design Center (FEDC) initiated a program in FY 81 directed towards the development of a Fusion Engineering Device (FED) tokamak design description. During the period from October 1980 to March 1981, the emphasis was on trade and design studies, in an effort to establish a baseline concept for the FED. This was followed by a period extending through September 1981 during which the chosen concept was examined in detail, and substantial progress was made towards a self-consistent FED design. The purpose of this paper is to describe the evolution of the poloidal field configuration in this design process, including the choice of an equilibrium field (EF) coil concept (Section 2), and the operating scenario of a particular coil set based on that concept (Section 3).

The method of particle and impurity control chosen for the FED baseline concept was that of a mechanical pump limiter. Part of the FED design philosophy, however, was to retain promising options in the case of major and unproven components, and in this area a poloidal divertor was identified as a primary alternative. In Section 4 we suggest a possible modification of the EF coil system that is consistent with a single-null poloidal divertor, and simulate its operation during a typical FED pulse. In Section 5 we examine a possible inconsistency between the baseline impurity control and the poloidal field configuration in the current FED, having to do with the sensitivity of the separatrix location to variations in plasma profiles and coil configurations, and suggest a feasible solution.

2. Choice of Baseline Configuration

Based on MHD stability studies[1,2] it is considered desirable for the plasma to be elongated ($\kappa = 1.6$) with a strong D shape ($\delta = 0.5$). These requirements in practice imply rather stringent design conditions. For example, a triangularity of $\delta = 0.5$ leads to the necessity of equilibrium field (EF) coils on the inboard side of the torus carrying large ampere-turns (~ 10 MA).

Three possible arrangements to position these inboard EF coils in a hybrid coil system[3] have been examined. As shown in Fig. 1, concept 1 with EF coils placed between the OH solenoid and the inner leg of the TF coil, superimposes the EF and the OH solenoid field at the end of a burn cycle. With the maximum ampere-turns specified by current drive and plasma equilibrium, a field of about 10 T is produced at the solenoid, exceeding the 8 T design limit of NbTi superconducting operated at 4°K.

Option 2 has a split OH solenoid, leaving space near the midplane for the inboard EF coils. This reduces the solenoid size and requires addition of nulling coils with large opposing currents to reduce stray OH fields at the plasma. In this case the voltsecond capability for startup becomes doubtful. Finally, option 3 of positioning inboard EF coils internal to the TF coils was rejected because of severe maintenance problems. None of these options appear acceptable from an engineering standpoint.

*Research sponsored by the Office of Fusion Energy, U.S. Department of Energy, under contract W-7405-eng-26 with Union Carbide Corporation.

By reducing the proposed plasma triangularity to about $\delta = 0.3$, inboard EF coils may be eliminated at the expense of larger shaping coil currents. Several feasible coil concepts were then identified (Fig. 2). These concepts were assessed by comparing the coil current requirements for the same degree of accuracy in plasma shaping.

The external flux $\psi^{(e)}$ distribution of a high-beta ($\langle\beta\rangle = 5.5\%$) FED plasma triangularity $\delta = 0.3$ and elongation $\kappa = 1.6$ was first obtained from numerical MHD equilibria by assuming an idealized set of coils. For any given set of admissible coil locations, currents c_j can then be calculated by finding a minimum of the quantity

$$w = \sum_i [\psi_i^{(e)} - \psi_i(\vec{c})]^2 + \alpha \sum_j c_j^2 , \qquad (1)$$

where the data $\psi_i^{(e)}$ is given on the plasma boundary and $\psi_i(\vec{c})$ are the corresponding values of poloidal flux created by the coil currents. Coil locations and the smoothing parameter α were varied until the field errors become acceptable.

$$\sum_i [\psi_i^{(e)} - \psi_i(\vec{c})]^2 / \sum_i \psi^{(e)2}_i < \varepsilon .$$

Approximate coil currents so obtained are given in Fig. 2 for $\varepsilon = 2.5 \times 10^{-4}$.

Based on analyses of cost and maintenance requirements[3] for the coil systems shown, the second option [Fig. 2(b)] consisting of normal internal shaping coils and superconducting external vertical field coils was chosen as the baseline concept. Coil locations consistent with the device configuration were then determined using the above methods. Because of space and access considerations, they are asymetric with respect to the plasma midplane.

3. Poloidal Field Configurations for Pumped Limiter

A sequence of equilibrium calculations were carried out to verify that the baseline coil configuration is appropriate in producing the field null required for startup, and to properly position and shape the plasma through the different stages of a typical 8 T FED discharge cycle (see Fig. 3). The coil currents resulting from the equilibrium calculations are compiled to simulate the current waveforms of the various coil groups (see Table 1 and Fig. 4).

A field null is required at time $t = 0$ to facilitate initiation of the plasma current channel in a minor radius of 0.4 m. Initially, non-zero currents are introduced in the EF coils for this purpose. A low-beta, circular plasma of minor radius 1 m is then established at $t = 2$ s. The plasma is maintained in contact with startup limiters at the outboard midplane. At $t = 6$ s the primary OH current has completed a swing from 60 MA to -30 MA, and an elongated, D-shape plasma in contact with the pumped limiter is formed. Auxiliary heating is assumed during the next six seconds, increasing beta to $\langle\beta\rangle = 5.5\%$, followed by a 100-s burn.

The current swing in the center section of the solenoid is accelerated for $3 \text{ s} \leq t \leq 6$ s. This has the effect of a split solenoid (option 2 in Fig. 1) without decreasing the voltsecond capability. Small variations are introduced in the EF coil currents during burn to cancel the solenoid stray field. The maximum current in all EF coils is less than 20 MA.

A desirable feature of the FED would be the possibility of a limited number of pulses with the TF coils operating at 10 T maximum field, and a similar analysis of the baseline PF coil operation scenario was carried out for this option, assuming the same current swing in the OH solenoid. It is seen that about a 25% increase in EF coil currents is needed for the 10 T option.

4. Poloidal Field Configurations for Poloidal Divertor

A single null poloidal divertor is proposed as the primary backup method of particle and impurity control for the FED. The poloidal field coil system in this case needs to be different from that of the baseline configuration because of somewhat increased current requirements necessary for separatrix control. A sequence of equilibria is computed for a possible poloidal divertor EF coil system, in order to model the plasma shapes and determine the coil current waveforms of a discharge cycle. The results are shown in Table 2 and Fig. 5.

The assumed discharge cycle scenario including startup, heating, and burn states is unchanged from that of the baseline. The coil arrangement shown in Fig. 5a represents a compromise accounting for limited access to interior coils, the need to provide neutron shielding and some degree of separatrix control, and the avoidance of excessively large coil currents. The use of normal, internal coils carrying limited current (~1 MA) results in significant reduction in currents from an all external system such as the current INTOR concept.[3] These coils could take the form of small coil loops within each torus segment[4] for maintenance purposes. The interior coils also help constrain the separatrix shift to $\lesssim$20 cm during plasma heating. Note that the plasma elongation and triangularity above the midplane is reduced to $\kappa = 1.5$ and $\delta = 0.2$ in order to obtain a connected scrapeoff region. As compared with the baseline system, relatively large superconducting coils and currents are needed in this case, resulting in a total EF current of $\gtrsim$30 MAT.

5. Poloidal Field Configuration Sensitivities

The proximity of the poloidal separatrix to the plasma edge may disconnect the plasma scrapeoff and seriously degrade the effectiveness of the pumped limiter. Thus, the dependence of separatrix location on the coil configuration and plasma parameters (e.g., κ and δ) needs to be clarified.

To ascertain this, an equilibrium code is used in which coil currents are iteratively adjusted in order to approximate a given plasma shape. The sensitivity of the flux lines in the scrapeoff region to the coil configuration, plasma parameters, and plasma shape are then examined. With the baseline coil concept, Fig. 6a shows that the separatrix for the near baseline plasma ($\langle\beta\rangle$ = 5.7%, B_t = 4.5 T, q_{edge} = 3.3, and I_p = 6.3 MA) is within the scrapeoff region, causing a large portion of the scrapeoff to be diverted before reaching the pumped limiter. Using a broader plasma current profile (Fig. 6b with I_p = 7.4 MA and q_ψ = 2.6) this situation is shown to improve, but the scrapeoff remains significantly disconnected.

Figure 7 exhibits the dependence of the separatrix and scrapeoff on the poloidal field coil system. The scrapeoff flux surfaces become fully connected (Fig. 7a) if inboard EF coils are used. When these inboard coils are removed (Fig. 7b), however, the resulting coil current distribution produces a separatrix close to the plasma boundary. Since Figs. 7b and Figs. 6a are similar, the proximity of separatrix is seen to

depend primary on the absence of inboard EF coils and not strongly on the number of EF coils or the plasma current profile. As a result, the poloidal flux lines are directed between the solenoid and the shaping coils, which carry current in an opposite direction through most of the discharge, forcing the null point toward the plasma.

Since the solenoid is an indespensible component in the design configuration, and given the engineering restrictions on the use of inboard EF coils, the solution to the problem of maintaining nested flux surfaces in the limiter region appears to be in a modification of the plasma shape. Figure 8 shows a case with connected scrapeoff region with a plasma elongation of $\kappa = 1.5$ and triangularity $\delta = 0.2$, using the baseline coil concept.

6. Conclusions and Future Work

A baseline coil concept (Fig. 3a) consisting of internal copper shaping coils and external, superconducting vertical field coils has been selected for FED design studies as a result of plasma equilibrium, engineering, and cost considerations. Numerical equilibrium calculations verify that this system is consistent with a baseline plasma shape of $\kappa = 1.6$ and $\delta = 0.3$. However, it is also shown that, in the absence of inboard EF coils, these shape parameters may be inconsistent with the impurity control configurations of pumped limiter and single null poloidal divertor. Reducing the elongation and triangularity $\kappa = 1.5$ and $\delta = 0.2$, respectively, is shown to permit an adequate scrapeoff region for their operation. If, in fact, it is necessary to modify the baseline plasma shape, the positions of the shaping coils are expected to vary from those of the current baseline. These locations, together with the exact number of shaping coils, will need to be ascertained. Another area that should be explored is that of the physics implications of employing asymmetric coil locations.

References

1. Y-K. M. Peng et al., Phys. Fluids 21 (1978) 467.
2. A. M. M. Todd et al., Nucl. Fusion 19 (1979) 743.
3. Y-K. M. Peng et al., in Proc. 7th Symp. on Eng. Problems of Fusion Research (1977) 186.
4. Fusion Engineering Design Center Staff, "FED Preconceptual Design Description," to be published as ORNL/TM-7948.
5. International Tokamak Reactor, Phase 1, to be published by the IAEA.

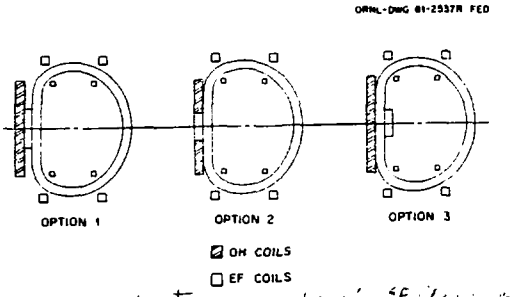

Figure 1. ~~The mega~~ ampere-turns ~~in the inboard EF coil bundle and OH solenoid~~ at the end of a burn cycle are indicated.

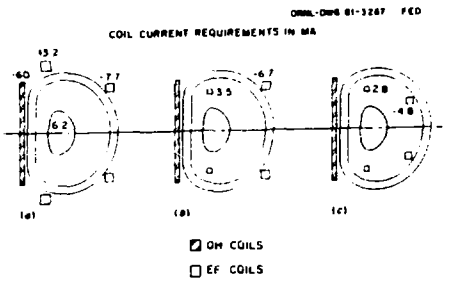

Figure 2. PF coil concepts omitting the inboard EF coils: (a) all exterior superconducting coils, (b) interior normal shaping coils, and (c) all interior normal coils. Coil ampere-turns at the end of the burn pulse are indicated.

PLASMA AND COIL CURRENT WAVEFORMS*

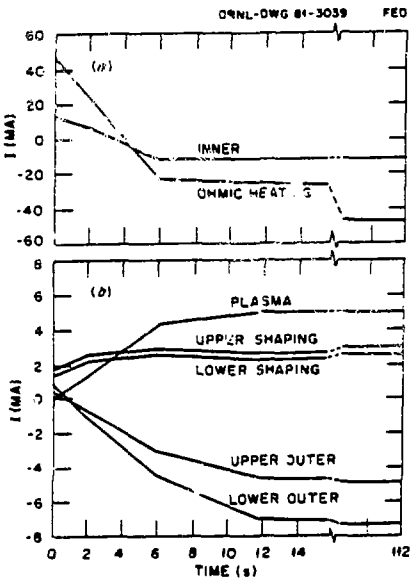

* ELONGATION = 1.6, TRIANGULARITY = 0.3, B_t = 5.6 T

Figure 4. Plasma and coil current waveforms for the 8 T operation with plasma parameters shown in Table 1.

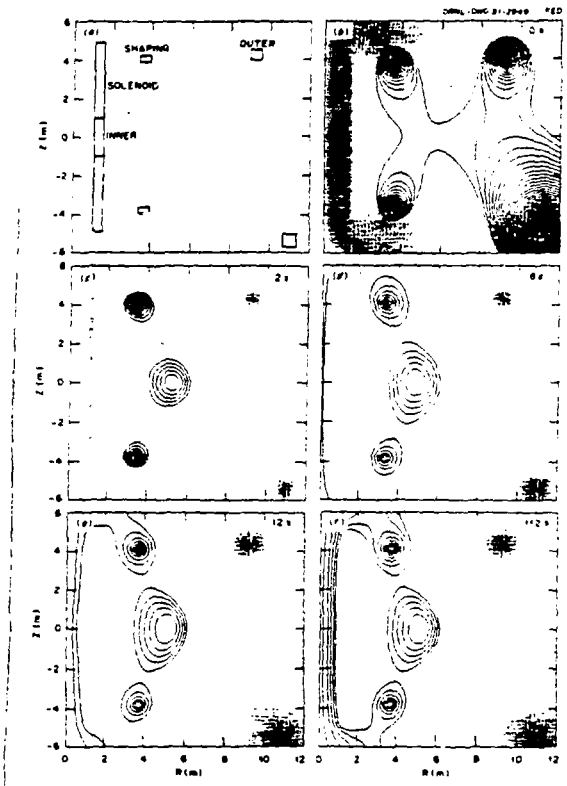

Figure 5. (a) Baseline poloidal field coil configuration and a typical sequence of poloidal flux plots at (b) t = 0 s, (c) t = 2 s, (d) t = 6 s, (e) t = 12 s, and (f) t = 112 s with plasma parameters given in Table 1.

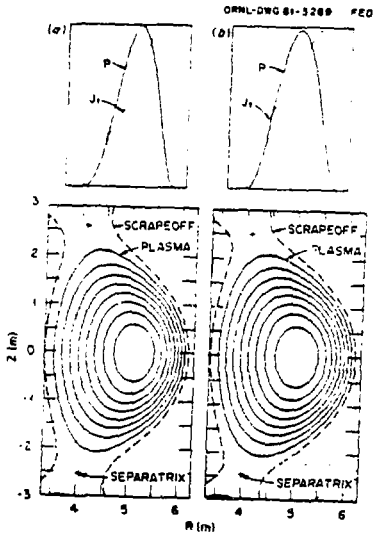

Figure 6. Using the baseline EF coil concept, the plasma scrapeoff region are disconnect by the presence of contained separatrix for (a) narrow and (b) broad plasma current profiles J_t.

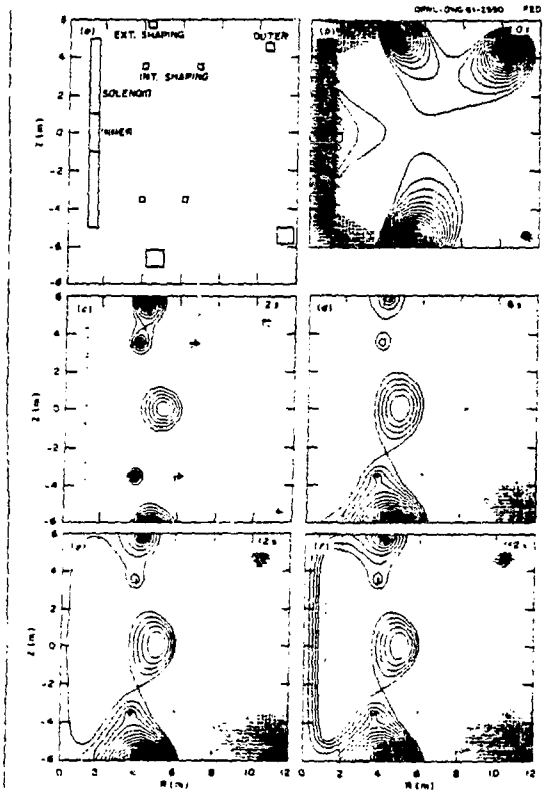

Figure 5. (a) Poloidal field coil configuration for the poloidal divertor option and a typical sequence of poloidal flux plots at (b) t = 0 s, (c) t = 2 s, (d) t = 6 s, (e) t = 12 s, and (f) t = 112 s with plasma parameters given in Table 2.

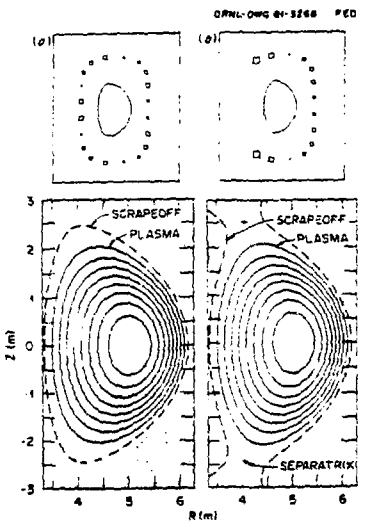

Figure 7. The closure of the scrapeoff flux surface is (a) obtained by the use of inboard EF coils and (b) lost in their absence, despite the addition of several EF coils.

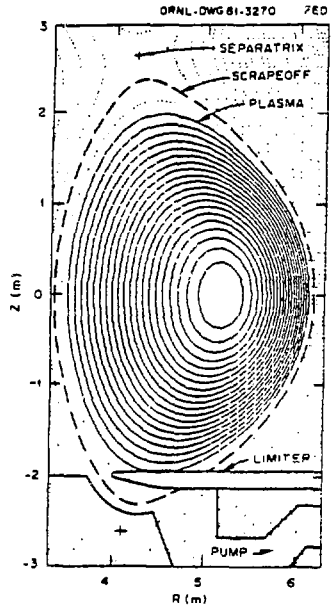

Figure 8. Using the baseline coil configuration, the scrapeoff flux surface becomes closed by reducing the triangularity and elongation to $\delta = 0.2$ and $\kappa = 1.5$.

Table 1
Example Plasma Parameters and Coil Current Requirements for the 8-T Operation (B_t = 3.6 T) with Pumped Limiter

Time into discharge(s)	0	2	6	12	112
Plasma shape					
Major radius (m)		5.1	4.8	4.8	4.8
Minor radius (m)		1.0	1.3	1.3	1.3
Elongation, κ		1.19	1.64	1.65	1.65
Triangularity, δ		0.07	0.28	0.43	0.36
Plasma parameters					
$\langle\beta\rangle$ (%)		0.49	0.40	5.55	5.54
q_{axis}		1.0	1.0	0.9	0.9
q_{edge}		3.4	3.5	3.7	3.7
I_p (MA)		1.4	4.4	5.0	5.0
Coil currents (MA)					
OH solenoid	48.0	24.0	-24.0	-25.0	-48.0
Inner coils	12.0	6.0	-12.0	-12.0	-12.0
Upper D-coil	1.8	2.9	2.9	2.6	3.0
Lower D-coil	2.0	2.5	2.6	2.3	2.6
Upper outer coil	0.6	-0.8	-3.1	-4.6	-4.8
Lower outer coil	1.0	-1.1	-4.5	-7.0	-7.3

Table 2
Example Plasma Parameters and Current Requirements for the 8-T Operation with Poloidal Divertor

Time into discharge(s)	0	2	6	12	112
Plasma shape					
Major radius (m)		5.09	4.80	4.85	4.85
Minor radius (m)		1.02	1.30	1.25	1.25
Elongation, κ		1.08	1.68	1.66	1.67
Plasma parameters					
$\langle\beta\rangle$ (%)		0.49	0.44	6.37	6.39
q(axis)		0.9	0.9	0.8	0.8
q(edge)		3.4	∞	∞	∞
I_p (MA)		1.4	4.4	5.0	5.0
Coil currents (MA)					
OH solenoid	48.0	24.0	-24.0	-25.4	-48.0
Inner coils	12.0	6.0	-12.0	-12.0	-12.0
Upper shaping (ext.)	2.4	2.6	1.3	2.4	2.5
Upper shaping (int.)	0.0	1.0	1.0	1.0	1.0
Lower shaping (ext.)	3.3	3.1	9.2	10.8	11.6
Lower shaping (int.)	0.0	1.0	1.0	1.0	1.0
Upper outer (ext.)	0.4	-0.6	-0.5	-2.6	-2.7
Upper outer (int.)	0.0	-1.0	-1.0	-1.0	-1.0
Lower outer (ext.)	0.2	-0.4	-7.9	-10.4	-11.1
Lower outer (int.)	0.0	-1.0	-1.0	-1.0	-1.0